Influence of thermal stratification on seasonal net ecosystem production and dissolved inorganic carbon in a shallow subtropical lake

Hao-Chi Lin [1], Chih-Yu Chiu [2], Jeng-Wei Tsai [3], Wen-Cheng Liu [4], Kazufumi Tada [5], and Keisuke Nakayama [a*]

[1] Graduate School of Engineering, Kobe University, 1-1 Rokkodai-cho Nada-ku, Kobe city, 658-8501, Japan.

[2] Research Center for Biodiversity, Academia Sinica, 128 Academia Road, Section 2, Nankang, Taipei 11529, Taiwan.

[3] Department of Biological Science and Technology, China Medical University, No. 91, Xueshi Road, North District, Taichung, 40402, Taiwan.

[4] Department of Civil and Disaster Prevention Engineering, National United University, No.2, Lien Da, Nan Shih Li, Miao-Li 36003, Taiwan.

[5] Chuden Engineering Consultants, 2-3-30 Deshio, Minami-ku, Hiroshima 734-8510, Japan.

[*] Corresponding author: Keisuke Nakayama (nakayama@phoenix.kobe-u.ac.jp)

Key Points:

- Typhoon plays a great role in dramatic release of carbon in a shallow lake.
- A model is presented to evaluate NEP by using residence time in a lake.
- Estimates of DIC demonstrate the importance of simulating stratification in a lake.

Abstract

Thermal stratification is a key physical process controlling carbon flux from lakes to the atmosphere. Vertical profiles in shallow subtropical lakes can vary greatly because typhoons frequently induce vertical mixing across the entire lake due to strong winds and rapid river flushing from inputs. Since carbon fluxes are driven by Dissolved Inorganic Carbon (DIC), it is necessary to clarify the effect of stratification on DIC dynamics in shallow subtropical lakes to estimate carbon fluxes. Therefore, we aim to clarify the influence of stratification on DIC in Yuan-Yong Lake that is a typical shallow subtropical lake. We measured the vertical profile of water temperature every month from July 2004 to December 2017. We applied a three-dimensional hydrological model to estimate net ecosystem production by combining with endmember analysis, suggesting the possibility that large amount of DIC is stored in the lower layer from spring to summer due to the suppression of vertical mixing by stratification. In autumn, DIC was diluted across the layers because of strong vertical mixing due to typhoons. Vertical profiles of DIC in winter were confirmed to be uniform due to overturning.

Plain Language Summary

Vertical profiles of dissolved inorganic carbon (DIC) is one of the most important factors to understand carbon emission from lakes. Thermal stratification is expected to be the key physical process controlling the vertical profile of DIC. To clarify the relationship between DIC and thermal stratification, we investigated vertical profiles of DIC and the strength of stratification in a subtropical shallow lake (Yuan-Yong lake, YYL) by using field observation data sets from 2004 to 2017. Our study is the first to apply a three-dimensional hydrological model to clarify the mechanism of the occurrence of the vertical distribution of DIC in order to estimate net ecosystem production in a lake.

1 Introduction

Freshwater ecosystems release substantial carbon to the atmosphere: approximately 0.3 to 1.8 Pg C yr^{-1} (Aufdenkampe et al. 2011; Engel et al. 2018; Lauerwald et al. 2015; Raymond et al. 2013). Small lakes (lake area < 0.1 km^2) occupy 25 to 35 % of the total area of all lakes in the world (Downing et al. 2006; Verpoorter et al. 2014). However, carbon emissions from small lakes are usually ignored when evaluating carbon fluxes (Cole et al. 2007; Raymond et al. 2013), which may result in the underestimation of carbon emission on a global scale (Downing et al. 2006; Verpoorter et al. 2014). In addition, lake size has been revealed to be one of the most important factors controlling carbon emissions, with small lakes having the larger contribution of convection to gas transfer velocity (Read et al. 2012; Vachon & del Giorgio et al. 2014). Rain storms and cooling-induced mixing are the most important meteorological forcing producing vertical mixing in small lakes and affect mass transport due to internal waves in a stratified shallow lake (Kimura et al. 2012 & 2017). Therefore, to accurately estimate carbon fluxes from small lakes it is necessary to clarify the mechanisms of vertical mixing and the breakdown of stratification.

There are many mountainous shallow lakes in subtropical East Asia. For example, in Taiwan, previous studies have showed that seasonal and annual carbon fluxes are frequently influenced by typhoon and monsoon events, but carbon fluxes from subtropical lakes above an altitude of 1,500 m are not well understood (Jones et al. 2009; Tsai et al. 2008, 2011, and 2016).

The typhoon season is from July to October and typhoons contribute to 10 % to 37 % of annual precipitation (Lai et al. 2006; Tsai et al. 2011). Typhoon-induced rapid flushing can mix the entire water in a small subtropical lake, with the thermal stratification likely to be destroyed (Kimura et al. 2012 and 2014; Shade et al. 2010; Tsai et al. 2008). Also, it has been demonstrated that strong typhoon disturbances alter water levels, water quality, lake metabolism, and CO2 fluxes in shallow subtropical lakes (Chiu et al. 2020; Jones et al. 2009; Tsai et al. 2008, 2011, & 2016). Jones et al. (2009) showed that the frequency of typhoons had the greatest impact on CO_2 fluxes in a shallow subtropical lake, increasing fluxes by approximately 2,200 kg C yr^{-1} per typhoon event. On the other hand, an absence of precipitation may affect the CO_2 dynamics across the air-water interface in subtropical lakes (Chiu et al. 2020; Xu & Xu et al. 2018). Long-term investigations of shallow subtropical lakes, such as at seasonal and annual scales, are rare and valuable. Additionally, carbon fluxes are not well understood in the freshwater ecosystems of subtropical lakes, especially in lakes located at high elevations over 1,500 m. Thus, investigation of shallow and small lakes in subtropical regions is necessary to clarify their physical structure in order to estimate carbon fluxes accurately.

CO_2 concentrations can be estimated from water temperature, salinity, Dissolved Inorganic Carbon (DIC) and pH or Total Alkalinity (TA) (Cai & Wang 1998; Smith 1985). If calcification is ignored, DIC is principally associated with the partial pressure of CO_2 (pCO_2) (Bade et al. 2004; Striegl et al. 2001). Previous studies showed that carbon fluxes in boreal lakes were mainly derived from DIC inputs (McDonald et al. 2013; Weyhenmeyer et al. 2015). In general, DIC concentrations in the epilimnion are lower than in the hypolimnion in a stratified lake due to photosynthesis dramatically decreasing pCO_2 in the epilimnion during the day (Guber et al. 2000). Also, mineralization of dissolved organic carbon (DOC) (Kortelainen et al. 2006) and carbonate deposition (or dissolution) in sediments at the lake bottom (Einsele et al. 2001) are associated with turbulence from wind shear (MacIntyre et al. 2001) and convective mixing (Eugster et al. 2003), which affect CO_2 flux. Therefore, the separation of the epilimnion and hypolimnion due to thermal stratification is one of the key physical processes controlling carbon flux in a lake (Åberg et al. 2010; Andersen et al. 2019; Eugster et al. 2003).

Irradiance and thermal stratification affect chemical activity, biological activity and physical transport in lakes (Imberger et al. 1985). Vertical mixing is an especially vital physical process in a stratified lake because it controls biochemical fluxes (Boehrer & Schultze, 2008; Gudasz et al. 2010; MacIntyre et al. 1993 and 2002). River flows and wind turbulence diffuse the biotic and abiotic materials from sediments into the water column (Andersen et al 2017; Boehrer & Schultze 2008; Czikowsky et al. 2018; Hope et al. 2004; MacIntyre et al. 1993& 2002). Allochthonous carbon is the main resource in a lake that facilitates ecosystem production (Lu et al. 2015; McDonald et al. 2013; Vachon & del Giorgio 2014). Therefore, the hydrological effect of carbon sources on the vertical profile of DIC in a lake needs to be understood through consideration of disturbances due to river inflows and wind. Water temperature is the key factor controlling the fate of carbon in shallow subtropical lakes. We thus aimed to investigate water temperature and DIC vertical profiles in order to quantify the seasonal mixing regime and seasonal pattern of vertical profiles of DIC for estimating net ecosystem production in a shallow subtropical lake.

2 Materials and Methods

105 2.1 Study site

106 Yuan-Yang Lake (YYL) is a typical shallow subtropical lake in East Asia, and YYL is
107 located in the Chi-Lan area of Yilan County in northern Taiwan (24°57'68" N, 121°40'22" E) at
108 an altitude of about 1,650 m (Figure 1). YYL is a natural lake and has been registered as a long-
109 term ecological study site by the National Science Council of Taiwan R.O.C. since 1992.
110 Additionally, YYL has been a part of the global lake ecological observatory network (GLEON)
111 since 2004. The air temperature around YYL ranges from -5 to 25℃ and annual precipitation
112 from 2,200 to 5,000 mm. About 40 % of the year is covered by heavy fog around YYL with
113 mean solar radiation of about 220 MJ m -2 17. YYL is a shallow alpine lake (surface area 3.6 ha
114 and water depth from 3.8 to 4.5 m) and the lake surface is ice-free all year round. YYL is
115 surrounded by pristine old-growth cypress forest, where the dominant tree species are
116 *Chamaecyparis formosensis*, *Chamaecyparis obtusa* var. *formosana*, and *Rhododendron*
117 *formosanum* Heiml. Aquatic plants exist around the lake, for instance, *Sparganium fallax* and
118 *Schoenoplectus mucronatus* subsp. *Robustus* are dominant species (Chou et al. 2000). The water
119 color is browning and humic with a mean of pH approximately 5.4 (Wu et al. 2001). The water
120 column is stratified from early April to October and usually well-mixed in winter from
121 December to February (Kimura et al. 2012).

122

123

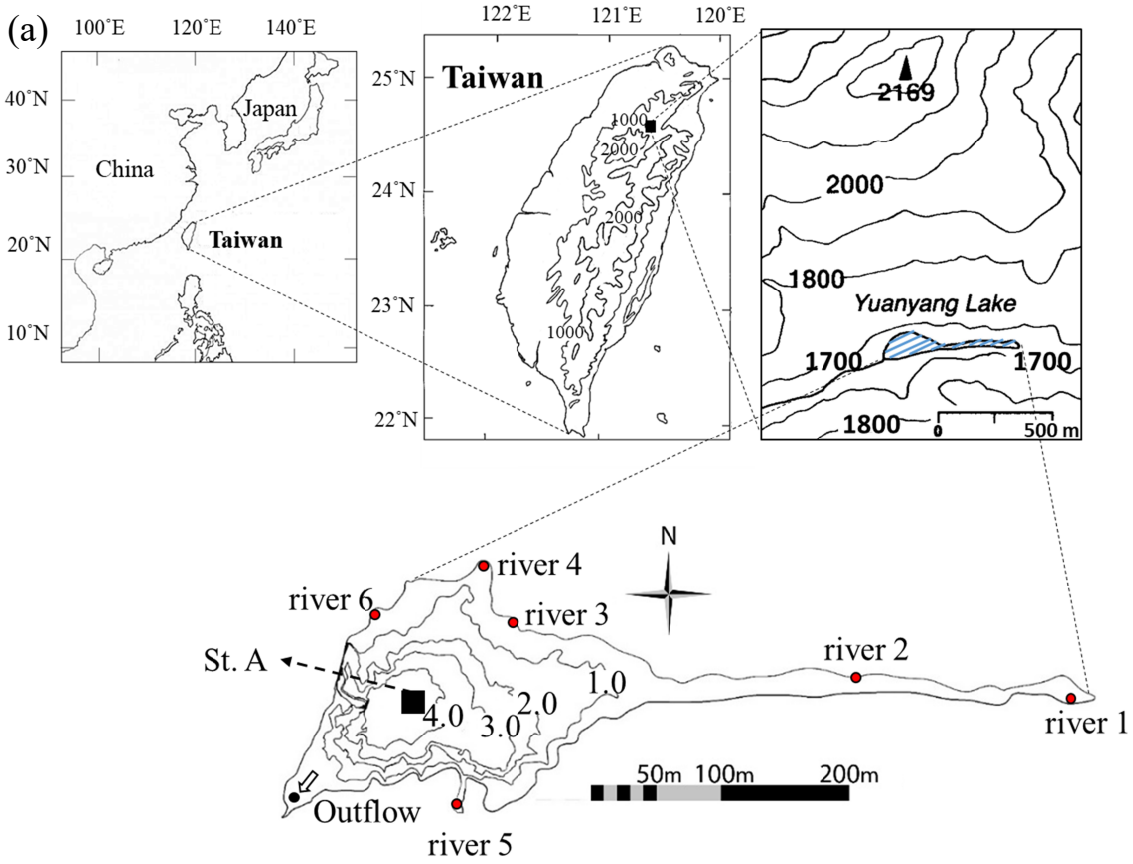

124

125 **Figure 1.** Location of Taiwan with an enlarged bathymetric map of Yuan-Yang Lake (YYL)
126 drawn with 1.0, 2.0, 3.0, and 4.0 m water depths contour lines. Station A (St. A) for vertical
127 profiles (Black Square), 6 river (Red circles) and outflow (Black circle) deployment sites.

128 2.2 Data collection

129 Water temperature was measured through the water column at water depths of 0.04, 0.25,
130 0.5, 0.75, 1.0, 1.5, 2, 2.5, 3.0, 3.5, and 4.0 m at St. A using a thermistor chain (Templine, Apprise
131 Technologies, Inc., Duluth, Minnesota, USA). The total water depth was measured at St. A once
132 or twice a month from July of 2004 to December of 2017 (Figure 1). Furthermore, we measured
133 the water surface temperature (0.04 m) of six inflow rivers and one outflow river (Figure 1).

134 We sampled water at St. A at water depths of 0.04, 0.5, 1.0, 2.0 and 3.5 m. In addition,
135 we sampled water at the water surface in six inflow rivers and one outflow river. The water
136 samples were filtered with plastic filters (47 mm GF／F; Whatman, Maidstone, Kent, UK) using
137 a portable hand pump (Hand Vacuum pump, One Lincoln Way, MO, USA). The water samples
138 were kept in airtight vials (Vial glass 40 ml, K60958A-912) that were stored in cooler box at
139 around 4 to 10℃ until analysis of dissolved inorganic carbon (DIC) concentrations less than 72
140 hours after sampling. We used a TOC analyzer (O. I. TOC analyzer 1010 from 2004 to 2012 and
141 model 1030W/1088 from 2013 to 2017, Xylem, TX, USA) and persulfate digestion to detect

142 DIC concentration by an infrared gas detector. We employed a sonar (LMS-332c GPS Receiver
143 and Sonar, Lowrance, USA) to measure bathymetry in August 2007 with a spatial interval of 1.0
144 m, which was used in the three-dimensional hydrological model.

145 We categorized the year into four seasons, spring (March to May), summer (June to
146 August), autumn (September to November) and winter (December to February). Since typhoons
147 cause great disturbance to the stratification in summer and autumn, we added two more
148 categories, summer typhoons (June to August) and autumn typhoons (September to November),
149 in order to explore how typhoons contribute to the vertical profile of water temperature and DIC.
150 It should be noted that mean duration of typhoon events was less than five days.

151 2.3 Brunt–Väisälä frequency, mixing depth and intrusion depth

152 We used the Brunt–Väisälä frequency (N, s^{-1}) to quantify the strength of stratification.
153 The Brunt-Väisälä frequency is associated with vertical mixing in a lake (von Rohden &
154 Imberger 2001).

$$N = \sqrt{-\frac{g}{\rho}\frac{d\rho}{dz}} \quad (1)$$

155 where g is the gravity, ρ is the density of water, and z is the vertical coordinate of water depth.

156 To define the depth of vertical mixing, mixing depth (Z_{mix}, m) was calculated following
157 Staehr and Sand-Jensen (2007) (Figure 2a).

$$Z_{mix} = Z|_{T = T_s - 1} \quad (2)$$

158 where Zmix is the mixing water depth, and TS is the water surface (0.04 m) temperature.

159 To know where river flow intrudes, we defined an intrusion depth (m), Zintru (Figure 2a).

$$Z_{intru} = Z|_{T = T_r} \quad (3)$$

160 where Tr is the water temperature from a river.

161

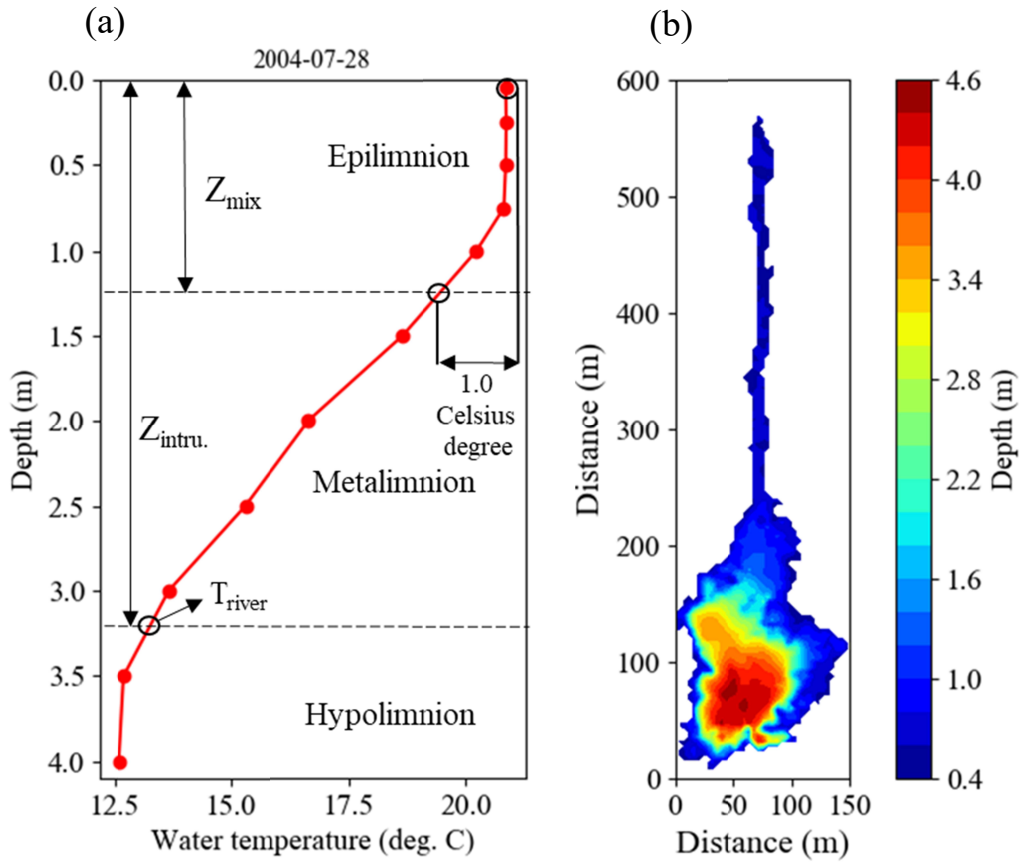

Figure 2. (a) Definition of intrusion depth (Zintru.) and mixing depth (Zmix). **(b)** Bathymetry in YYL. Triver is water temperature from the rivers.

To understand the relationship among the parameters, water temperature, Z, Zmix, Zintru, water surface DIC, hypolimnion DIC and river DIC, we performed a Spearman correlation (rs).

2.4 Net Ecosystem Production (NEP)

To estimate net ecosystem production, we used endmember analysis using DIC of the rivers (Christophersen et al. 1990; Hooper et al. 1990). Since there are 6 inflow rivers in YYL, mean DIC concentration (mg L^{-1}) of the inflow water was estimated as:

$$\mathrm{DIC}_R = \frac{\sum_{i=1}^{6} Q_i \mathrm{DIC_i}}{\sum_{i=1}^{6} Q_i} \quad (4)$$

where DIC_R is the mean DIC from rivers into YYL, DIC_i is the DIC from river_i and Q_i is the discharge of river_i (Dalrymple 1960; Laurenson 1965). Q_1 to Q_6 are 0.072, 0.009, 0.027, 0.018, 0.036 and 0.018 $m^3 s^{-1}$, respectively. measurements were only carried out after incident internal waves had reached the sloping boundary.

NEP is zero when there is no biological activity, which corresponds to the condition when DIC in YYL is the same as DIC_R (Tokoro et al 2014). When DIC in YYL is larger than DIC_R, carbon is produced in the lake which corresponds to a negative NEP. When DIC is smaller than DIC_R, carbon is absorbed into the lake, which corresponds to a positive NEP. Thus, the change in DIC due to photosynthesis and respiration is defined as

$$\Delta\mathrm{DIC} = \mathrm{DIC} - \mathrm{DIC}_R \quad (5)$$

We obtained ΔDIC in YYL using DIC at the water depth of 0.04 m, 0.5 m, 1.0 m, 2.0 m, and 3.5 m. As a result, NEP (mg C m^{-3} d^{-1}) can be obtained using residence time (d^{-1}) of YYL (Tokoro et al 2014).

$$\mathrm{NEP} = -(\Delta\mathrm{DIC}_{0.04\mathrm{m}}\mathrm{V}_{0.04\mathrm{m}} + \Delta\mathrm{DIC}_{0.5\,\mathrm{m}}\mathrm{V}_{0.5\mathrm{m}} + \Delta\mathrm{DIC}_{1\,\mathrm{m}}\mathrm{V}_{1\mathrm{m}} + \Delta\mathrm{DIC}_{2\,\mathrm{m}}\mathrm{V}_{2\mathrm{m}} + \Delta\mathrm{DIC}_{3.5\mathrm{m}}\mathrm{V}_{3.5\mathrm{m}})/(t_r\,\mathrm{V}_{\mathrm{total}}) \quad (6)$$

where $V_{0.04m}$, $V_{0.5m}$, $V_{1m,}$ V_{2m} and $V_{3.5m}$ are the volume at each water depth (Table 1), Vtotal is the total volume (Table 1), and tr is the residence time of YYL.

Table 1. Vertical profile of water volumes in YYL

Variables	Region of water depth (m)	Volume (m^3)
$V_{0.04m}$	0.0 – 0.5 m	18,000
$V_{0.5m}$	0.5 – 1.0 m	6,640
V_{1m}	1.0 – 1.5 m	5,114
V_{2m}	1.5 – 2.5 m	7,488
$V_{3.5m}$	2.5 – 4.0 m	3,360
V_{total}	0.0 – 4.0 m	40,602

To estimate the residence time in YYL, we performed three-dimensional hydrological simulations using a three-dimensional environmental model, Fantom3D, which is based on object-oriented programming methods (Laniak et al., 2013; Maruya et al., 2010; Nakamoto et al., 2013; Nakayama et al., 2012, 2014, 2016, & 2019). For numerical simulations, the initial vertical profiles of mean water temperatures and mean DIC concentrations were obtained for typical stratified conditions for each season (Figure 3). The grid size of horizon mesh was 4.0 m and the vertical grid size was 0.2 m. The time step was 0.5 s. The residence time (tr) was estimated from the temporal change in tracer concentrations.

3 Results

3.1 Water temperature and DIC in YYL.

Mean water surface temperature was the highest in summer at 19.1 °C, with the difference in water temperature between the water surface (0.04 m) and bottom (4.0 m) around 10.8 °C at this time (Figure 3b). Mean water surface temperature in winter was the lowest at 11.3 ºC (Figure 3d). Mean water temperatures adjacent to the bottom were 8.5, 12.7, 12.9, and 8.7 °C from spring to winter, respectively (Figure 3a-3d). Although mean water surface temperatures during summer typhoon were lower than normal summer conditions, mean water surface temperatures during autumn typhoon were higher than normal autumn conditions (Figure 3b, 3c, 3e & 3f).

Mean water surface DIC was about 3.0 mg L-1 during spring to summer and about 2.5 mg L-1 during autumn to winter (Figure 3a to 3d). Mean water surface DIC during autumn typhoon was the lowest observed (Figure 3e & 3f). YYL stored larger DIC concentrations in the hypolimnion (3.5 m) compared to water surface during spring to autumn (Figure 3a - 3c). Mean hypolimnion DIC in summer was the largest, at 7.5 mg L-1, although mean DIC during summer typhoons were vertically uniform and only about 2.5 mg L-1 (Figure 3b & 3e). Mean hypolimnion DIC in winter was also low, at 2.8 mg L^{-1}, due to vertical mixing and the lowest prevailing water temperatures (Figure 3d). The vertical profile of mean DIC was almost uniform after typhoons (Figure 3e & 3f).

Mean river temperatures were the highest in summer, 15.1 ºC, and lowest in winter, 10.7 ºC (Figure 4a). The difference in water temperature between lake surface water and the rivers was at its highest in spring and summer. River DIC in spring and summer was also higher than at other times (Figure 4b). Mean river DIC in summer was the highest, 3.7 mg L^{-1}, and that after autumn typhoons was the lowest, 1.8 mg L^{-1} (Figure 4b).

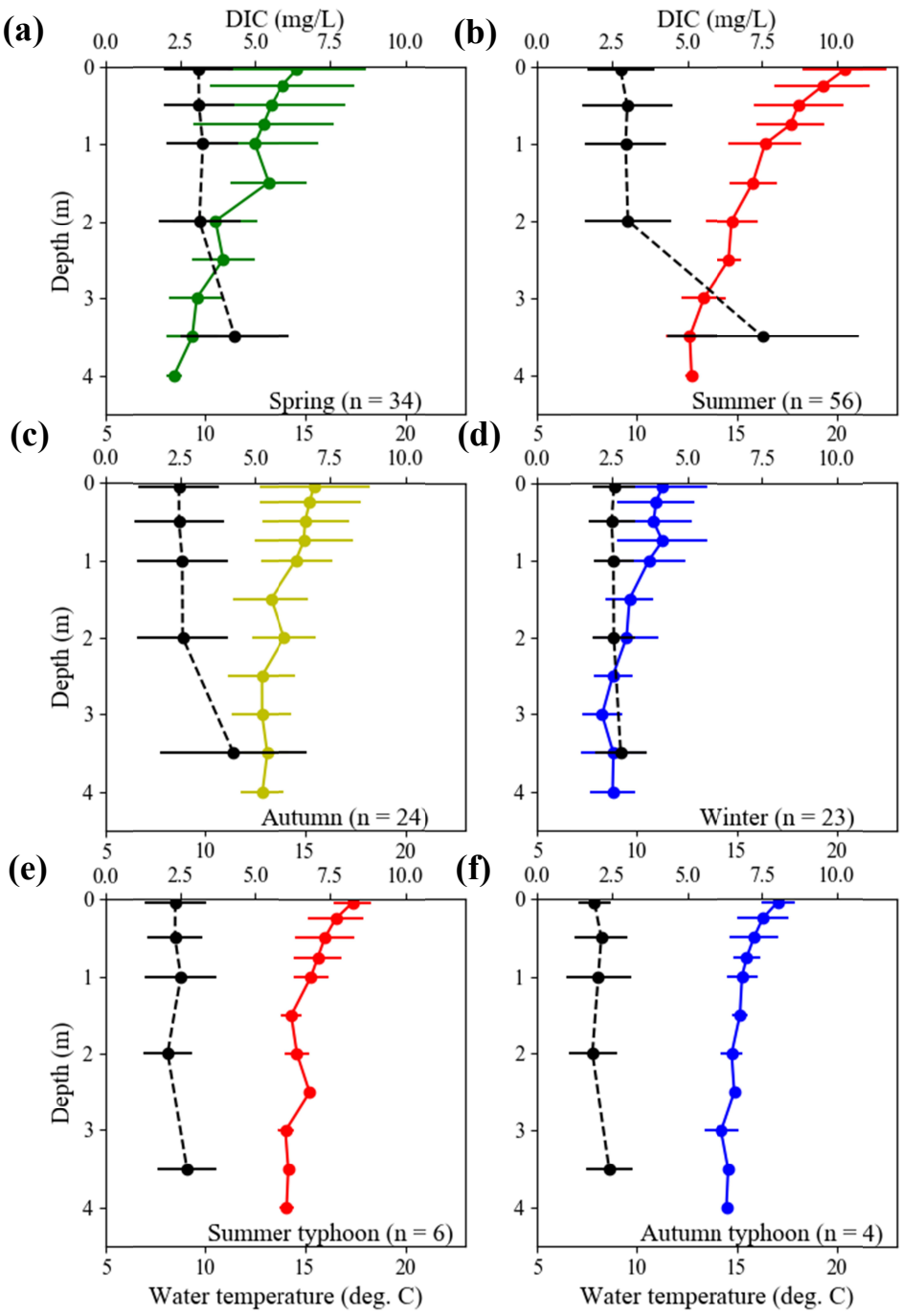

Figure 3. Overview of the vertical profiles of mean water temperature (colors solid lines) and DIC (black dashes) during **(a)** spring, **(b)** summer, **(c)** autumn **(d)** winter **(e)** summer typhoons **(f)** autumn typhoons over the period July 2004 to December 2017. The dots show mean value, the horizontal lines standard deviation (n is samples size).

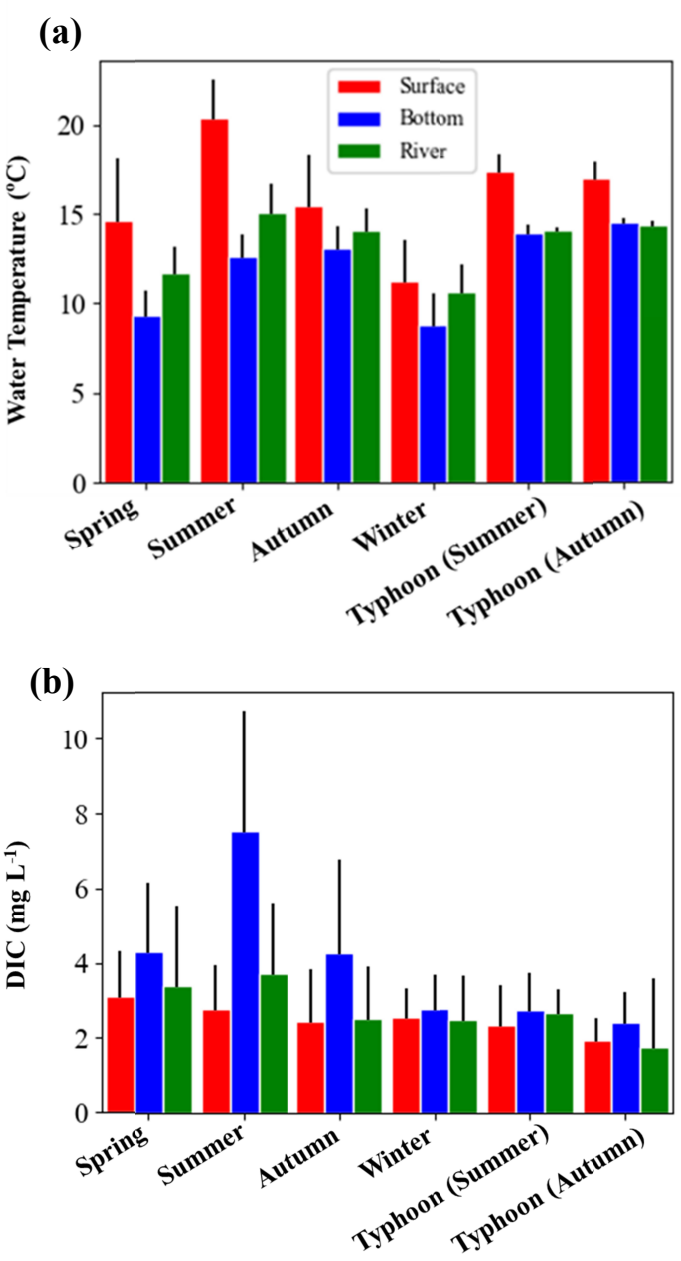

Figure.4. Comparison of **(a)** water temperatures and **(b)** DIC concentrations among surface (0.04 m, red bars), bottom (3.5 m, blue bars), and river water (Triver and DICR, green bars). The color bars show mean values and black solid line the standard deviations.

3.2 Mixing depth, Brunt-Väisälä frequency, and Intrusion depth

Mixing depths were less than 25 % of the total water depth (Figure 5a). Mean mixing depth was the largest in winter (25 % of water depth) and was the smallest in summer (7.5 %; Figure 5a). Mean Brunt-Väisälä frequency ranged between around 0.006 and 0.013 s-1; in summer it was twice as much as when it was at its lowest in autumn (Figure 5b). In other words,

the stratification in spring and summer were stronger than autumn and winter. The Brunt-Väisälä frequency after typhoons was higher than in autumn and winter (Figure 5b). Mean intrusion depth was about 50 % of the total water depth from spring to autumn, compared to 100 % of the total water depth after typhoons (Figure 5c). In contrast, intrusion depth in winter was small, approximately 10 % of the total water depth (Figure 5c).

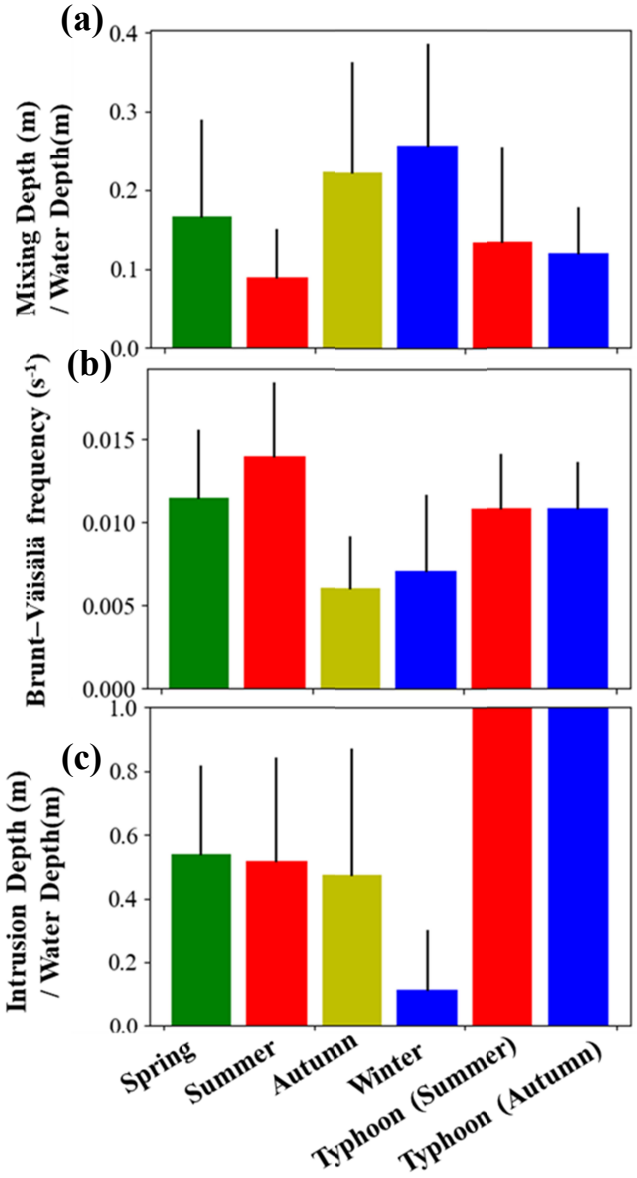

Figure 5. Comparison of the **(a)** mixing depth, **(b)** Brunt–Väisälä frequency, and **(c)** intrusion depth among the seasons in YYL. The color bar are mean values and the solid black lines the standard deviations. The intrusion depth and mixing depth are normalized by total water depths.

Water surface DIC was not clearly associated with water temperature (Figure 6a and Table 3). However, hypolimnion DIC and water temperature showed a significant positive correlation (rs = 0.61, $p < 0.001$) (Figure 6b and Table 2). Hypolimnion DIC and river DIC had the strongest positive correlation (rs = 0.69, p < 0.001) (Figure 6c and Table 2). Hypolimnion DIC and river DIC showed a positive correlation with Brunt-Väisälä frequency (rs = 0.43 & 0.32, $p < 0.001$) (Figure 6e & 6f), but water surface DIC was not clearly association with water temperature and Brunt-Väisälä frequency (Figure 6a & 6d and Table 2). Brunt-Väisälä frequency and mixing depth were associated with water surface temperature (Figure 6g, 6h & Table 2) with high spearman correlation coefficients (rs = 0.64 & 0.40, $p < 0.001$). Despite the observation that Brunt-Väisälä frequency and mixing depth had the strongest absolute correlation (rs = - 0.88, $p < 0.001$) (Figure 6i), mixing depth did not have strong correlations with hypolimnion DIC and river DIC (Table 2). Intrusion depth had significant positive correlations with water temperature, Brunt-Väisälä frequency, and hypolimnion DIC (rs = 0.58, 0.32, 0.32, respectively, p < 0.001, Table 2). In contrast, intrusion depth was not association with mixing depth, water surface DIC, or river DIC (Table 2).

Table 2. Spearman correlation coefficients for DIC concentration, water temperature, Brunt-Väisälä frequency, and intrusion depth. BVF is Brunt-Väisälä frequency. WT (0.04 m) is water surface temperature.

Variables	Mixing depth	BVF	DIC (surface)	DIC (Hypo.)	DIC (river)	Intrusion depth
WT (0.04 m)	-0.398*** (122)	0.643*** (142)	0.029 (142)	0.611*** (142)	0.31** (76)	0.581*** (66)
Mixing depth		-0.879*** (122)	0.115 (122)	-0.221 (122)	-0.158 (66)	-0.155 (52)
BVF			0.017 (142)	0.427*** (142)	0.324*** (76)	0.324*** (66)
DIC (surface)				0.438*** (152)	0.32*** (84)	0.162 (66)
DIC (Hypo.)					0.686*** (84)	0.321*** (66)
DIC (river)						-0.005 (31)

269

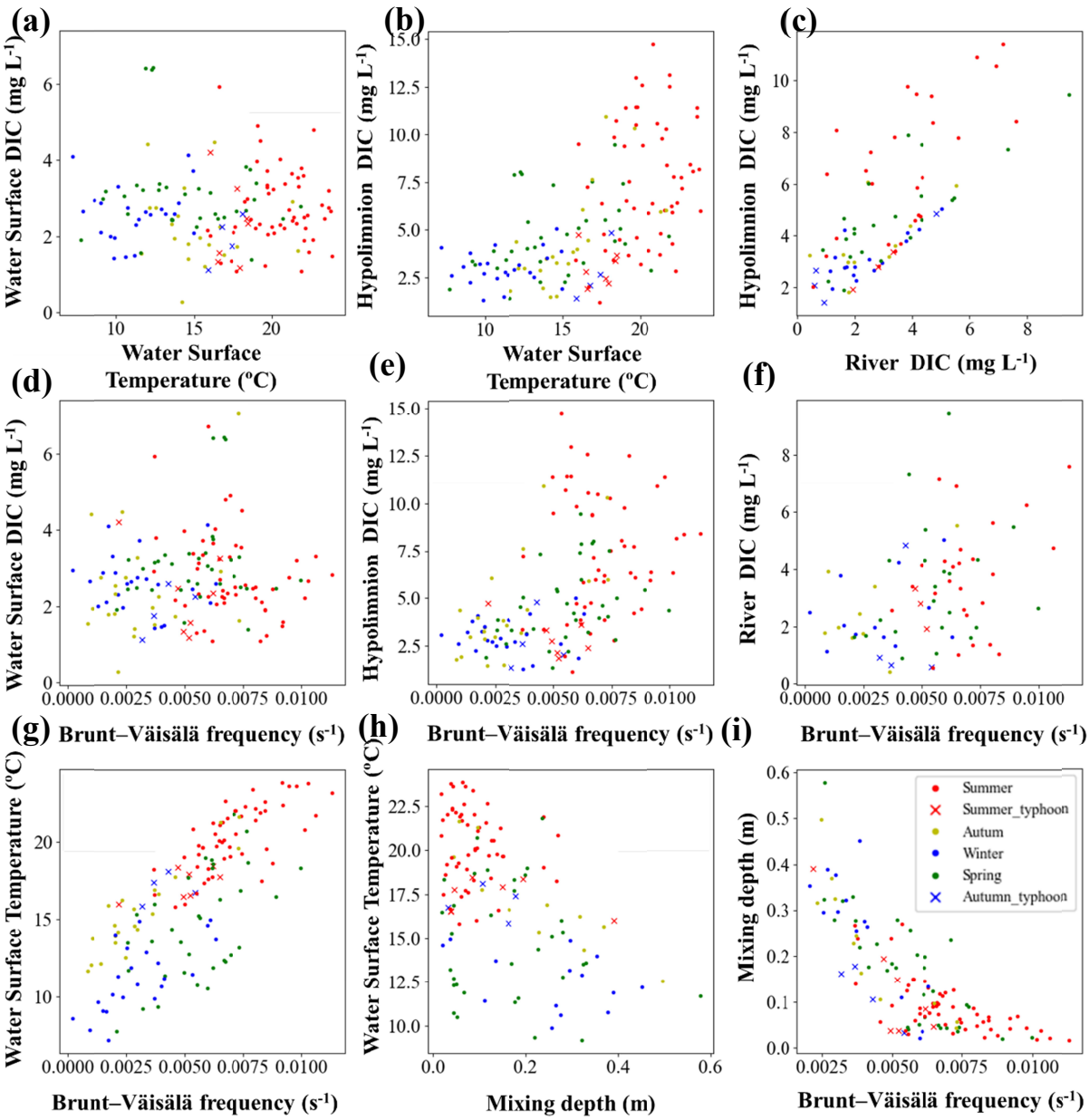

270

271 **Figure 6.** Relationship between water surface temperatures and **(a)** water surface DIC. **(b)**
272 Hypolimnion DIC, **(g)** Brunt–Väisälä frequency, **(h)** mixing depth; **(c)** is relationship between
273 Hypolimnion DIC and River DIC; and relationship between Brunt–Väisälä frequency and **(d)**
274 water surface DIC, **(e)** Hypolimnion DIC, **(f)** River DIC, **(i)** mixing depth. The green points
275 show spring data; red points the summer data; yellow points the autumn data; blue points the
276 winter data; red crosses the summer typhoon data; and the blue crosses the autumn typhoon data.

277

278

279 3.3 Water temperature and DIC in YYL.

280 The absolute mean of ΔDIC in the upper layer in spring and summer was lower than
281 autumn (Figure 7a to 7c). Mean lower layer ΔDIC in spring (0.83 mg L^{-1}) was lower than
282 autumn (1.86 mg L^{-1}), and mean ΔDIC in summer was the highest at 3.82 mg L-1. Mean ΔDIC
283 in the upper layer in autumn was the highest, around 1.0 mg L-1, while the absolute value of
284 mean ΔDIC was the lowest in winter, about 0.06 mg L^{-1} (Figure 7c and 7d). Mean upper layer
285 ΔDIC in summer was smaller compared to summer typhoon (Figure 7b & 7e). In contrast to
286 summer, mean upper layer ΔDIC in autumn was larger than during autumn typhoons (Figure 7c
287 & 7f).

288

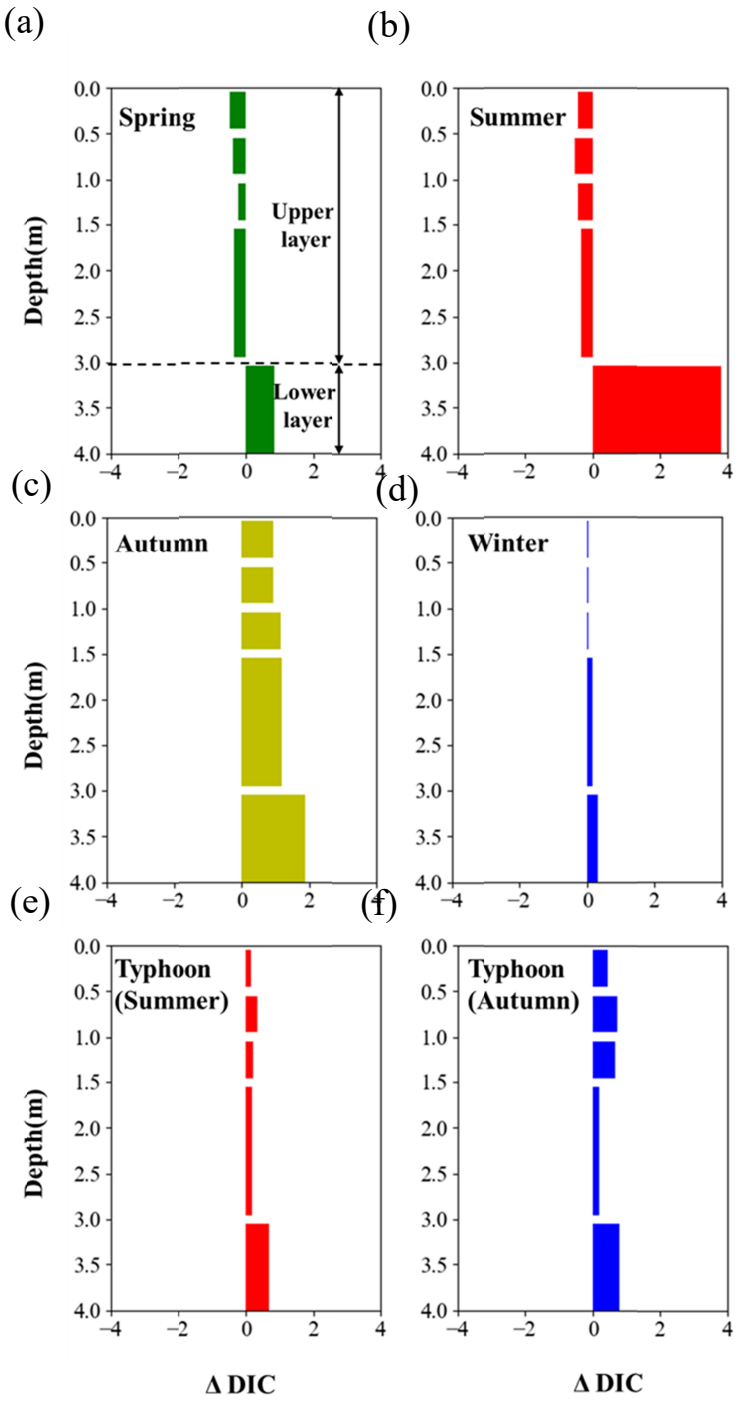

Figure 7. Mean vertical profiles Δ DIC during (a) spring, (b) summer (c) autumn (d) winter (e) summer typhoons, and (f) autumn typhoons.

To obtain the residence time of YYL for the estimation of NEP, numerical computations were carried out by giving uniform initial tracer concentration with the value of 1.0 (Figure 8a). River flow intrudes into the middle layer in YYL due to the stratification effect on the second day after the initial condition (Figure 8b). Since the intrusion causes vertical mixing, a large tracer concentration area adjacent to the bottom was reducing on the third day relative to the

297 second (Figure 8c). Finally, residence time for the four seasons was estimated by giving typical
298 stratified conditions for each season (Table 3). As spring and summer have the stronger
299 stratification compared to autumn and winter, the residence time was longer in spring and
300 summer than autumn and winter. As expected, residence time in winter was the shortest at 1.3
301 days. NEP was 114.3 (mg C m^{-3} d^{-1}) and 33.7 (mg C m^{-3} d^{-1}) in spring and summer, respectively,
302 but NEP in autumn and winter was negative (Figure 9). The absolute value of NEP in autumn
303 was the largest with a NEP of -674.5 mg C m^{-3} d^{-1}.

304

305 **Table 3.** The estimated residence time (tr) among seasons.

Variables	Spring	Summer	Autumn	Winter	Unit
t_r	2.6	2.6	1.7	1.3	days

306
307

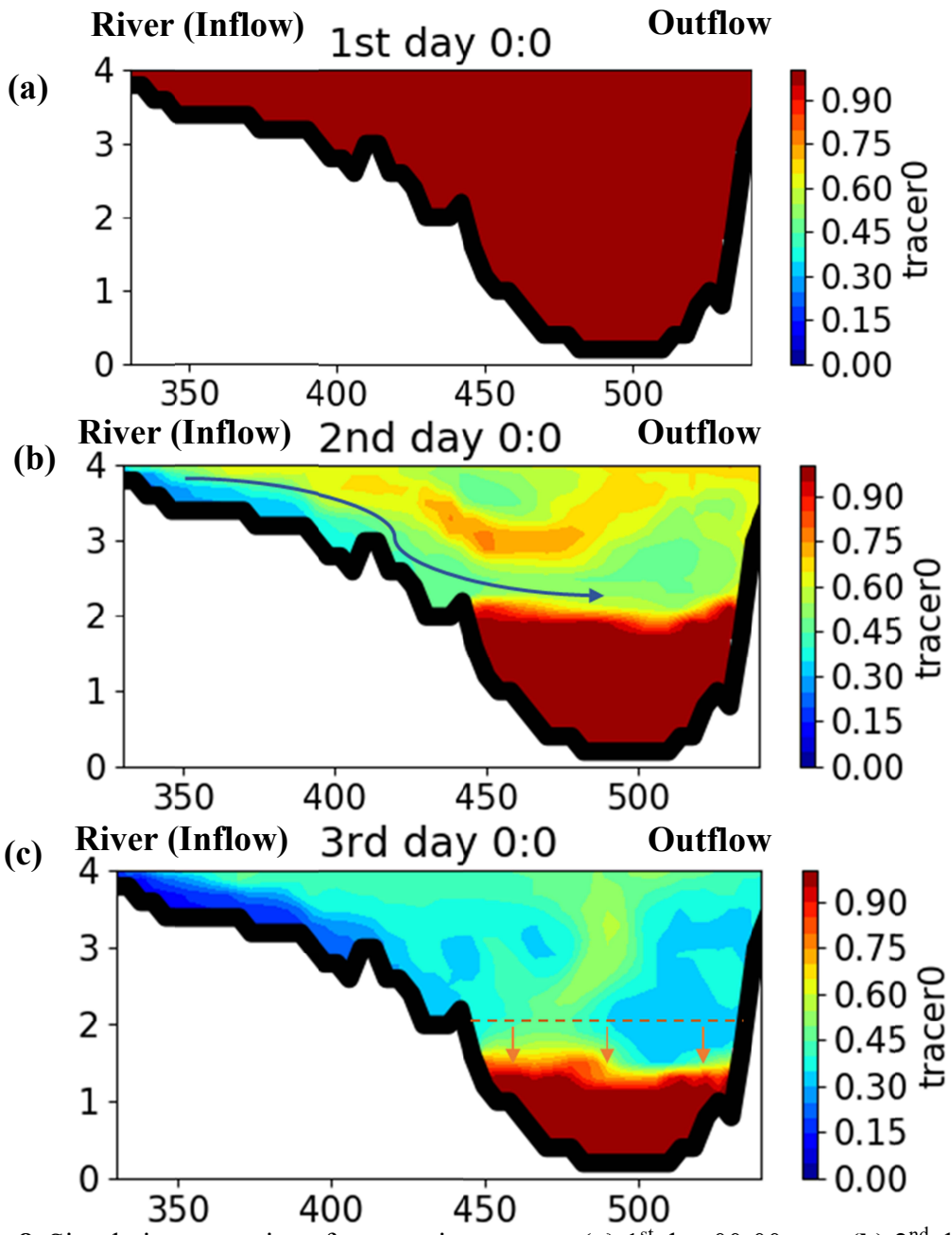

Figure 8. Simulation scenarios of a tracer in summer. **(a)** 1st day 00:00 a.m. **(b)** 2nd day 00:00 a.m. **(c)** 3rd day 00:00 a.m. X-axis is horizontal distance (m); Y-axis is water depth (m) from bottom to water surface. Contour are drawn to show the concentration of the tracer.

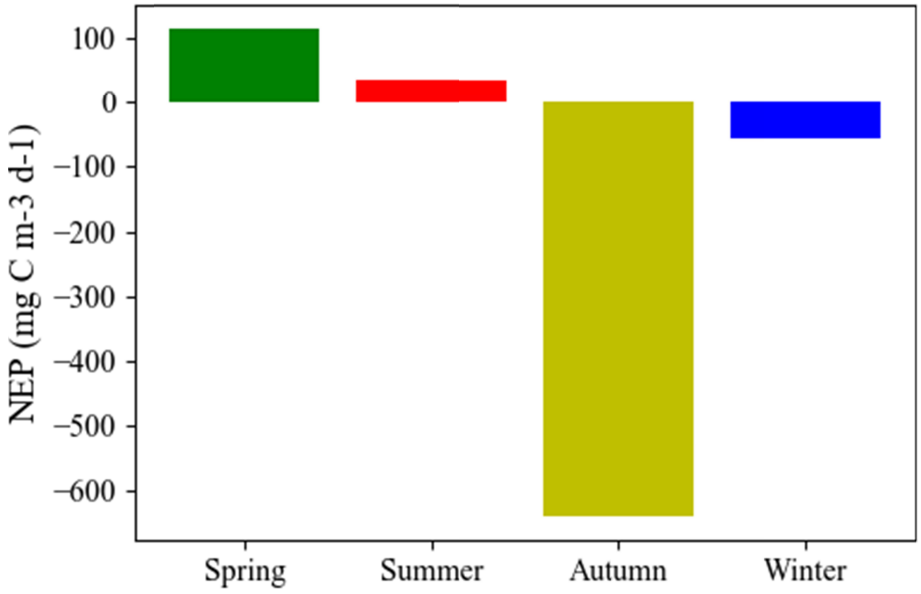

Figure 9. Contribution of NEP in YYL (excluding the typhoon periods). Carbon is absorbed when NEP > 0 was; carbon releases when NEP < 0.

4 Discussion

In this shallow subtropical lake stratification was stronger in spring and summer (mean N were 0.011 s^{-1} & 0.013 s^{-1}) compared to autumn and winter (mean N were 0.0006 s^{-1} & 0.0007 s^{-1}). Typhoons induced large flushing from rivers, which resulted in the generation of weak stratification. Strong stratification inhibits vertical DIC transport from the lower to the upper layer, which results in negative ΔDIC in the upper layer from spring to summer due to the predominance of photosynthesis (Figure 7a & b). Strong thermal stratification during spring to summer drives longer residence times than in the autumn to winter (Table 3). Spearman correlations showed strong correlations between Brunt-Väisälä frequency and DIC in the hypolimnion (Figure 6e & Table 2). NEP in summer was lower than spring (Figure 9) because the absolute value of mean ΔDIC in the lower layer was 10 times larger than the upper layer in summer (Figure 7a & 7b). In contrast, the stratification in autumn was weaker than spring and summer. Therefore, the DIC stored in the lower layer was vertically diluted up to the water surface easily, which resulted in the largest production of carbon in YYL (Figure 7c). NEP dramatically decreased from summer to autumn due to weak stratification (Figure 9). In winter, although vertical mixing is strong because there is no stratification, the absolute value of ΔDIC was small since ecological production is at its lowest due to the low water temperature.

Previous studies demonstrated that thermal stratification was a major driver affecting pCO_2 and CO_2 fluxes (Åberg et al. 2010; Andersen et al. 2019; Vachon & del Giorgi 2014). Precipitation and storm events played a particularly strong role when they flushed large concentrations of terrestrial DIC into the lake, which then released CO_2 and CH_4 (Bartosiewicz

et al. 2015; Hope et al. 2004; Tonetta et al. 2017; Vachon & del Giorgi 2014;). In our dataset there are 10 typhoon events, all of which occurred in summer and autumn (Table 4). Although the strength and frequency of typhoons were different between summer and autumn (Table 4), our results showed the vertical profile of DIC and water temperature were well-mixed after all typhoons (Figure 3b, 3c, 3e & 3f). Because each typhoon event led to large precipitation events relative to the annual precipitation, the stratification became very weak after each typhoon (Fig 3e & 3f). Kimura et al. 2012 applied the Lake Number (von Robertson & Imberger 1994, L_N) to quantify the vertical mixing in YYL, which suggested that the water column was mixed completely ($L_N < 1$) during typhoons and the winter. Wind shear and convective mixing play a large role in diurnal heat flux in a lake (Imberger 1985). When the water column is mixed by typhoons, the heat flux was found to decrease dramatically in YYL (Kimura et al. 2014). Czikowsky et al. (2018) demonstrated that the duration of well-mixed conditions due to storms was around 1 to 2 days in Lake Pleasant, which resulted in a 50 % decrease in heat flux compared with the strongly stratified period. Previous studies suggested that storm events may impact CO_2 fluxes (Liu et al. 2016; Tonetta et al. 2017; Vachon & del Giorgio. 2014). Emissions of CO_2 across the air-water interface due to seasonal cooling-induced mixing have been shown to be larger than storm-induced mixing (Czikowsky et al. 2018). Our analysis revealed that CO_2 emissions were the largest in autumn because typhoons occur frequently and the water column is well-mixed. It thus seems necessary to consider the long-term effects of typhoons on CO_2 emissions in addition to seasonal changes.

To understand how much CO_2 is released from a lake to the atmosphere and is absorbed from the atmosphere into a lake, we applied Fick's law to obtain the air-water CO_2 gas exchange 63 (Table 5). Mean CO_2 emissions ranged from 35.8 to 47.7 mg C m^{-2} d^{-1}, and mean pCO_{2water} was around 564 to 662 μatm (Table 6). Carbon emissions in YYL were confirmed to be similar to those in shallow temperate lakes (Aufdenkampe et al. 2011; Raymond et al. 2013). In winter, water temperatures (11.05 ± 1.92 °C), DIC (2.20 ± 0.43 mg L-1) and KCO_2 (1.85 ± 0.42 m s-1) were lowest, which leads to lower mean F_CO2 than spring and autumn. Mean F_CO2 in summer was the lowest (131.2 mg CO_2 m^{-2} d^{-1}) because of the strong stratification (Figure 3b & 5b). Our results showed that mean F_{CO2} in autumn is the highest (207.4 mg CO_2 m^{-2} d^{-1}) due to the supply of DIC from the lower to the upper layer under the condition of weak stratification (Figure 3c & 5b). Large standard deviation of DIC from summer to autumn was associated with a large standard deviation in F_{CO2}due to high frequency typhoons (Tables 4 & 6). Therefore, we suggest that that not only large loading of allochthonous carbon from the surrounding forest but also storm events influence carbon emission in a shallow lake (Chiu et al. 20020; Hope et al. 2004; Shade et al. 2009; Sobek et al., 2003; Tsai et al. 2008).

375 **Table 4. Characteristics of precipitation and wind speed between summer and autumn typhoon periods during 2004 to 2017.**

Typhoon Name	Date	Sampling date	Total precipitation (mm)	Maximum daily precipitation (mm)	Maximum wind speed (m s-1)	Ranking
Summer typhoons (Total 56 typhoon events)						
201513SOUDELOR	7-9 Aug. 2015	-	355.5	304.0	49.7	3rd/81
200708SEPAT	16-19 Aug.2007	22-24 Aug.2007	266.2	129.6	27.8	16th/81
200417AERE	23-26 Aug.2004	31 Aug. 2004	283.9	232	34.1	4th/81
200509MATSA	3-6 Aug. 2005	9 Aug. 2005	227.4	127	31.2	18th/81
200505HAITANG	16-20 Jul. 2005	20 Jul.2005	248.7	120.5	36.8	20th /81
Autumn typhoons (Total 25 typhoon events)						
200813SINLAKU	12-15 Sep.2008	20 Sep. 2008	552	355.5	44.7	2nd /81
201013MEGI	21-23 Oct. 2010	25 Oct. 2010	501.9	356.5	16.6	1st /81
200513TALIM	1 Sep. 2005	5 Sep. 2005	149	149	39.5	13th /81
200712WIPHA	17-18 Sep. 2007	20 Sep. 2007	85.3	59.5	16.3	33th /81

376 The data refer to typhoon data base of Central Weather Bureau in Taiwan. The meteorological station located in Yilan CWBT
377 station (24°76'39" N, 121°75'65" E).
378 Ranking is followed maximum daily precipitation of typhoons events. 201513SOUDELOR was the best ranking in summer.
379

380 **Table 5.** Equations and references of CO_2 flux (F_{CO2}) across the air–water interface. Measured data was located St. A.

Variables	Equation	References & equipment
F_{CO2}	$k_{CO2} \cdot K_H(pCO2_{water} - pCO2_{air})$	Fick's law diffusion
$pCO2_{air}$ (CO2 partial pressure in the atmosphere)	Measured data · 390 (ppm)	Air pressure sensor (model 090D; Met One Ins., NW, U.S.A.)
$pCO2_{water}$	$\frac{DIC(10^{-pH})^2}{[(10^{-pH})^2 + (10^{-pH})K_1 + K_1K_2]K_H}$	Cai and Wang 1998
pH	Measured data	Water quality probe (Hydrolab 4α; Hach, CO, U.S.A.)
DIC	Measured data (DIC concentration, 0.04 m)	
k_{CO2} (Gas transfer velocity)	$k_{600}\left(\frac{Sc_{CO_2}}{600}\right)^{-0.67}$	Cole and Caraco 1998
k_{600} (Gas exchange coefficient)	$2.07 + 0.215\ U_{10}^{1.7}$	Jähne *et al*. 1987
Sc_{CO_2} (Schmidt number)	$1911.1 - 118.11\ T + 3.4527\ T^2 - 0.04132\ T^3$	Wanninkhof, 1992
U_{10}	$U_2 \cdot (\frac{10_{(m)}}{2_{(m)}})^{0.15}$	Smith, 1985
U_2	Measured data (Wind speed above water surface 2 m)	Wind monitor (model 05106; R.M. Young, MI, U.S.A.)
K_H (Henry's coefficient)	$\exp(108.39 + 0.0199\mathrm{T} - \frac{6920}{\mathrm{T}} - 40.452\log \mathrm{T} + \frac{669365}{T^2})$	Plummer and Busenberg, 1982
$\mathrm{K_1}$ (1st dissociation constant)	$\exp(-356.31 - 0.0609\mathrm{T} + \frac{21834}{\mathrm{T}} + 126.83\log \mathrm{T} - \frac{1684915}{\mathrm{T^2}})$	Plummer and Busenberg, 1982
$\mathrm{K_2}$ (2nd dissociation constant)	$\exp(-107.8 - 0.0325\mathrm{T} + \frac{5152}{\mathrm{T}} + 38.926\log \mathrm{T} - \frac{56371}{T^2})$	Plummer and Busenberg, 1982
T	Measured data (Water temperature (K), 0.04 m)	

Table 6. CO_2 flux in YYL during July 2011 to December 2017 (not including 2012 and 2013). *Fc* is carbon emission.

Variables	Unit	Spring	Summer	Autumn	Winter
n		12	18	12	12
WT	(°C)	15.59 ± 2.96	20.58 ± 1.87	15.72 ± 2.18	11.05 ± 1.92
K_{co2}	(m s^{-1})	2.23 ± 0.55	2.42 ± 0.33	2.35 ± 0.26	1.85 ± 0.42
pH		6.10 ± 0.84	5.78 ± 0.85	6.05 ± 0.58	6.25 ± 0.66
DIC	(mg L^{-1})	2.44 ± 0.54	2.31 ± 1.32	2.56 ± 1.70	2.20 ± 0.43
$pCO2_{air}$	(μatm)	331.6 ± 1.30	331.6 ± 1.05	332.4 ± 0.79	332.0 ± 0.52
$pCO2_{water}$	(μatm)	634.3 ± 147.1	563.7 ± 328.3	661.8 ± 429.3	608.8 ± 116.9
F_{CO2}	(mg CO_2 m^{-2} d^{-1})	167.3 ± 70.1	131.2 ± 186.2	207.4 ± 290.8	139.9 ± 62.9
F_C	(mg C m^{-2} d^{-1})	45.62 ± 19.13	35.77 ± 50.78	56.56 ± 79.30	38.17 ± 17.14

5 Conclusions

We categorized the seasonal pattern of stratification in a shallow subtropical lake as shown in Figure 10. In spring and summer, the stratification is strongest, which forms a clear three-layer system (Figure 10a). Although hypolimnion DIC is very high due to release from sediments at the lake bottom, strong stratification inhibits the vertical diffusion of the hypolimnion DIC into the epilimnion and metalimnion. This results in a reduction in DIC in the upper layer due to photosynthesis (Figure 10a). In autumn, although mean air temperatures were almost the same as spring (Lai et al. 2006), stratification became weaker due to vertical mixing by typhoons (Figure 10b). As a result, DIC is likely to be diffused from the lower to the upper layer. In addition, spearman correlations showed strong correlation between river DIC and hypolimnion DIC. The river DIC and the strength of stratification may thus control the vertical profile of DIC during spring to autumn. In contrast, the water column is vertically well-mixed in winter and river flow intrudes adjacent to water surface (Figure 10c). Moreover, foggy conditions reduced solar radiation in winter to less than about 150 J m-2 (Lai et al. 2006). Previous studies demonstrated the importance of low light for the limitation of biomass productivity in lake ecosystems (Mallin & Paerl 1992; Karlsson et al. 2009). Low water temperatures and light limitation affect ecosystem production and there would be limited biological activity expected in cold and dark conditions (Figure 10c). During summer and autumn typhoons river inflow into the bottom layer due to typhoon-induced mixing enhances the vertical mixing of river DIC in a shallow subtropical lake (Figure 10d).

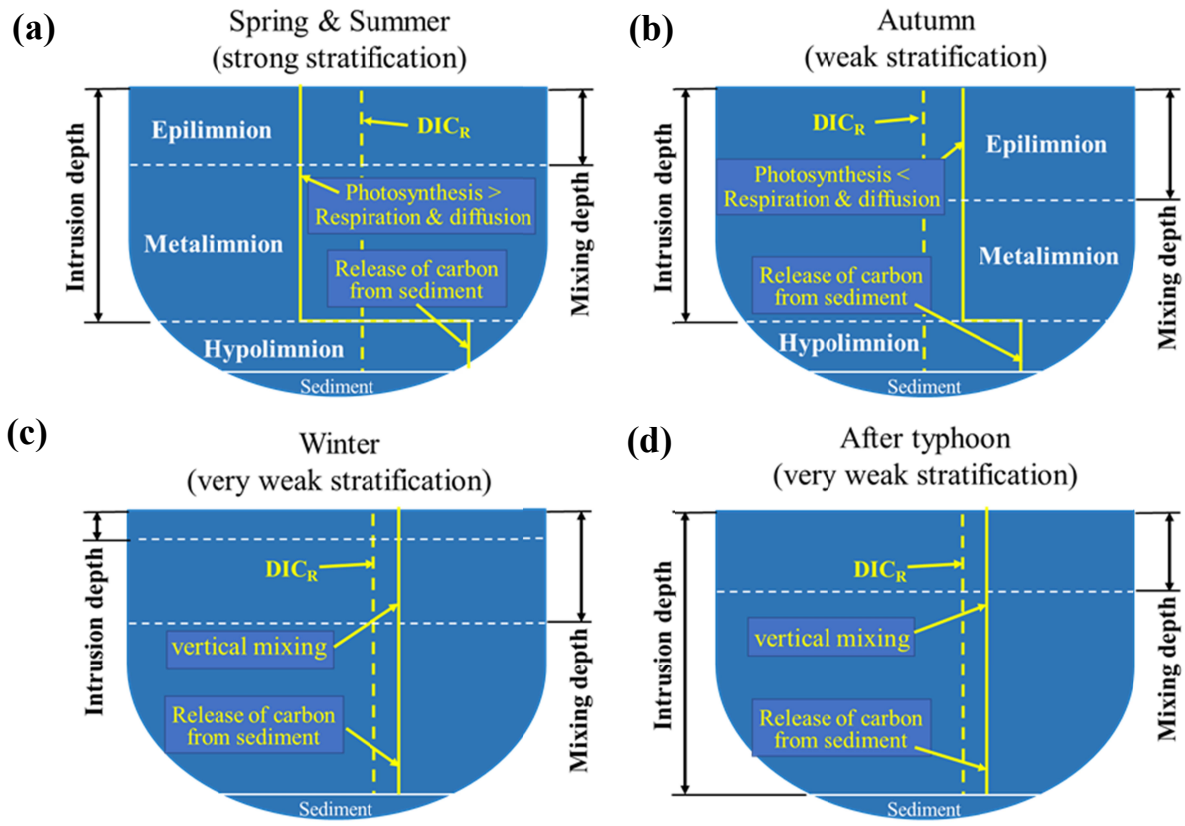

Figure 10. Schematic diagrams of stratification **(a)** in spring and summer **(b)** in autumn **(c)** in winter, and **(d)** after typhoons. The horizonal while-dash line is the boundary of stratification, the vertical yellow line is the DIC concentration, and the vertical yellow-dash line is DIC_R.

Acknowledgements

This work was supported by Taiwan National Science Council, Taiwan (NSC 94-2621-B-001-003, NSC 95-2621-B-001-001, and 97-2621-B-039-001-MY2), Ministry of Science and Technology, Taiwan (MOST 105-2621-B-039-001, MOST 107-2621-M-239-001), Academia Sinica, Taiwan (AS-103-TP-B15) for CY Chiu. We thank BS Lin, YL Chou, YS Hsueh, JY Liu, YX Lan, ZY Wu, YJ Miao, and LC Jiang for water samples collection and chemistry analysis, and the Japan Society for the Promotion of Science under grant 18H01545 and 18KK0119 for K Nakayama. This study benefited from participation in the Global Lakes Ecological Observatory Network (GLEON). The executable binary (windows, Mac, Linux) of the three-dimensional hydrodynamic model, Fantom, used in this study, is available from http://www.comp.tmu.ac.jp/shintani/fantom.html. The model outputs are available from https://github.com/kuaqua/JGR2020BGS, "The model outputs for Lin et al. (2020)".

References

Åberg, J., Jansson, M, and Jonsson, A. (2010), Importance of water temperature and thermal stratification dynamics for temporal variation of surface water CO_2 in a boreal lake. *J. Geophys. Res. Biogeosci.*, 115, G02024. doi:10.1029/2009JG001085.

Andersen, M. R., Sand-Jensen, K., Iestyn Woolway, R, and Jones, I. D. (2017), Profound daily vertical stratification and mixing in a small, shallow, wind-exposed lake with submerged macrophytes. *Aquat Sci.*, 79(2), 395–406. doi:10.1007/s00027-016-0505-0.

Andersen, M. R., Kragh, T., Martinsen, K. T., Kristensen, E., and K., Sand-Jensen., (2019), The carbon pump supports high primary production in a shallow lake. *Aquat Sci.*, 81(2), 24. doi:10.1007/s00027-019-0625-4.

Aufdenkampe, A. K., Mayorga, E., Raymond, P. A., Melack, J. M., Doney, S. C., Alin, S. R., Aalto, R. E., and Yoo, K. (2011), Riverine coupling of biogeochemical cycles between land, oceans, and atmosphere. *Front Ecol. Environ.*, 9(1):53–60. doi:10.1890/100014.

Bade, D. L., S. R. Carpenter, J. J. Cole, P. C. Hanson, and Hesslein, R. H. (2004), Controls of δ13C-DIC in lakes: Geochemistry, lake metabolism, and morphometry. *Limnol. Oceanogr.*, 49(4), 1160-1172. doi:10.4319/lo.2004.49.4.1160.

Bartosiewicz, M., I. Laurion, and S. MacIntyre. (2015), Greenhouse gas emission and storage in a small shallow lake. *Hydrobiologia*,757(1), 101-115. doi:10.1007/s10750-015-2240-2.

Boehrer, B., & Schultze, M. (2008), Stratification of lakes. *Rev. Geophy*., 14(2) 129-134. doi:10.1029/2006RG000210.

Cai, W. J.,& Wang, Y., (1998), The chemistry, fluxes, and sources of carbon dioxide in the estuarine waters of the Satilla and Altamaha Rivers, Georgia. *Limnol. Oceanogr.*, 43(4), 657-668. doi:10.4319/lo.1998.43.4.0657.

Chiu, C. Y., Jones, J. R., Rusak, J. A., Lin, H. C., Nakayama, K., Kratz, T. K., Liu, W. C, Tang, S. L., and Tsai, J. W. (2020), Terrestrial loads of dissolved organic matter drive inter-annual carbon flux in subtropical lakes during times of drought. *Sci. Total Environ.* 717:137052. doi: 10.1016/j.scitotenv.2020.137052.

Christophersen, N., Neal, C., Hooper, R. P., Vogt, R. D., and Andersen, S. (1990), Modelling streamwater chemistry as a mixture of soilwater end-members. A step towards second-generation acidification models. *J. Hydrol.* 116(1), 307-320.

Chou, C.H., Chen, T. Y., Liao, C. C., and Peng, C. I. (2000), Long-term ecological research in the Yuanyang Lake forest ecosystem I. Vegetation composition and analysis. *Bot. Bull. Acad. Sin.* 41(1), 61-72.

Cole, J. J., and Caraco, N. F. (1998), Atmospheric exchange of carbon dioxide in a low-wind oligotrophic lake measured by the addition of SF6. *Limnol. Oceanogr.*,43(4), 647-656. doi: 10.4319/lo.1998.43.4.0647.

Cole, J. J., Prairie, Y. T., Caraco, N. F., McDowell, W. H., Tranvik, L. J., Striegl, R. G., Duarte, C. M., Kortelainen, P., Downing, J. A., Middelburg, J. J., Melack, J. (2007), Plumbing the global carbon cycle: integrating inland waters into the terrestrial carbon budget. *Ecosystems*, 10(1), doi: 172-185. 10.1007/s10021-006-9013-8.

Czikowsky, M. J., MacIntyre, S., Tedford, E. W., Vidal, J., and Miller, M. D. (2018), Effects of Wind and Buoyancy on Carbon Dioxide Distribution and Air-Water Flux of a Stratified Temperate Lake. *Journal of Geophy Res. Biogeosci.*, 123 (8), 2305-2322. doi: 10.1029/2017JG004209.

Dalrymple, T. 1960. Flood-frequency analyses, manual of hydrology: Part 3 (No. 1543-A). USGPO.

Downing, J. A., Prairie, Y. T., Cole, J. J., Duarte, C. M., Tranvik, L. J., Striegl, R. G., McDowell, W. H., Kortelainen, P, Caraco, N. F, Melack, J. M., and Middelburg, J. J. (2006), The global abundance and size distribution of lakes, ponds, and impoundments. *Limnol. Oceanogr.*, 51(5), 2388-2397. doi:10.4319/lo.2006.51.5.2388.

Einsele, G., Yan, J., and Hinderer, M. (2001), Atmospheric carbon burial in modern lake basins and its significance for the global carbon budget. *Global Planet Change*, 30(3-4), 167-195. doi:10.1016/S0921-8181(01)00105-9.

Engel, F., Farrell, K. J., McCullough, I. M., Scordo, F., Denfeld, B. A., Dugan, H. A., de Eyto, E., Hanson, P .C., McClure, R. P., Nõges, P.; Nõges, T., Ryder, E., Weathers, K. C., and Weyhenmeyer, G. A. (2018), A lake classification concept for a more accurate global estimate of the dissolved inorganic carbon export from terrestrial ecosystems to inland waters. *Sci. Nat.*, 105(3-4), 25. doi:10.1007/s00114-018-1547-z.

Eugster, W., Kling, G, Jonas, T., McFadden, J. P., Wüest, A., MacIntyre, S., and Chapin III, F. S. (2003), CO_2 exchange between air and water in an Arctic Alaskan and midlatitude Swiss lake: Importance of convective mixing. *J. Geophy Res Atmos*, 108, D12. doi: 10.1029/2002JD002653.

GLEON Yuan-Yang Lake site, http://gleon.org/lakes/yuan-yang-lake.

Gruber, N., Wehrli, B., and Wüest, A. (2000), The role of biogeochemical cycling for the formation and preservation of varved sediments in Soppensee (Switzerland). *J. Paleolimnol.*, 24(3), 277-291. doi:10.1023/A:1008195604287.

Gudasz, C., Bastviken, D., Steger, K., Premke, K., Sobek, S., and Tranvik, L. J. (2010), Temperature-controlled organic carbon mineralization in lake sediments. *Nature*, 466(7305), 478-481. doi:10.1038/nature09186.

Hooper, R. P., Christophersen, N., and Peters, N. E. (1990), Modelling streamwater chemistry as a mixture of soil water end-members—An application to the Panola Mountain catchment, Georgia, USA. *J. Hydrol.*, 116(1), 321-343. doi:10.1016/0022-1694(90)90131-G.

Hope, D., Palmer, S. M., Billett, M. F., and Dawson., J. J. (2004), Variations in dissolved CO_2 and CH4 in a first-order stream and catchment: an investigation of soil–stream linkages. *Hydrol Processes*, 18(17), 3255-3275. doi:10.1002/hyp.5657.

Imberger, J. (1985), The diurnal mixed layer. *Limnol. Oceanogr.*, 30(4), 737-770. doi: 10.4319/lo.1985.30.4.0737.

Jähne, B., Münnich, K. O., Bösinge, R., Dutzi, A., Huber, W., and Libner, P. (1987), On the parameters influencing air-water gas exchange. *Journal of Geophysical Research: Oceans*, 92, 1937-1949. doi:10.1029/JC092iC02p01937.

Jones, S. E., Kratz, T. K., Chiu, C. Y., and McMahon, K. D. (2009), Influence of typhoons on annual CO_2 flux from a subtropical, humic lake. *Glob. Change Biol.*, 15(1), 243-254. doi: 10.1111/j.1365-2486.2008.01723.x.

Karlsson, J., Byström, P., Ask, J., Ask, P., Persson, L., and Jansson, M. (2009), Light limitation of nutrient-poor lake ecosystems. *Nature*, 460(7254), 506. doi:10.1038/nature08179.

Kimura, N., Liu, W. C., Chiu, C. Y., and Kratz, T. (2012), The influences of typhoon-induced mixing in a shallow lake. Lakes *Res. Res. Manag.*, 17(3), 171-183. doi: 10.1111/j.1440-1770.2012.00509.x.

Kimura, N., Liu, W. C., Chiu, C. Y., and Kratz, T. K. (2014), Assessing the effects of severe rainstorm-induced mixing on a subtropical, subalpine lake. *Environ. Monit. Assess*, 186(5), 3091-3114. doi:10.1007/s10661-013-3603-7.

Kimura, N., Liu, W. C., Tsai, J. W., Chiu, C. Y., Kratz, T. K., and Tai, A. (2017), Contribution of extreme meteorological forcing to vertical mixing in a small, shallow subtropical lake. *J. limnol.*, 76(1), 116-128. doi:10.4081/jlimnol.2016.1477.

Kortelainen, P., Rantakari, M. Huttunen, J. T., Mattsson, T., Alm J., Juutinen S., Larmola, T., Silvola, J., and Martikainen, P. J. (2006), Sediment respiration and lake trophic state are important predictors of large CO_2 evasion from small boreal lakes. *Glob. Change Biol.*, 12(8), 1554-1567. doi:10.1111/j.1365-2486.2006.01167.x.

Lai, I. L., Chang, S. C., Lin, P. H., Chou, C. H., and Wu, J. T. (2006), Climatic characteristics of the subtropical mountainous cloud forest at the Yuanyang Lake long-term ecological research site, Taiwan. *Taiwania*, 51(4), 317-329.

Laniak, G.F., Olchin, G., Goodall, J., Voinov, A., Hill, M., Glynn, P., Whelan, G., Geller, G., Quinn, N., Blind, M, Peckham, S., Reaney, S., Gaber, N., Kennedy, R., and Hughesm, A. (2013), Integrated environmental modeling: A vision and roadmap for the future. *Environmental Modelling and Software*, 39, 3-23. doi: 10.1016/j.envsoft.2012.09.006.

Lauerwald, R., Laruelle, G. G., Hartmann, J., Ciais, P., and Regnier. P. A. (2015), Spatial patterns in CO_2 evasion from the global river network. *Global Biogeochem Cycles*, 29 (5), 534-554. doi:10.1002/2014GB004941.

Laurenson, E. M. (1965), Storage routing methods of flood estimation. Inst. Eng. Aust. *Civ. Eng. Trans.* 39-47.

Liu, H., Zhang, Q., Katul, G. G., Cole, J. J., Chapin III, F. S., and MacIntyre, S. (2016), Large CO_2 effluxes at night and during synoptic weather events significantly contribute to CO_2 emissions from a reservoir. *Environ Res. Lett.* 11(6), 064001. doi: 10.1088/1748-9326/11/6/064001.

Lu, W., Wang, S., Yeager, K. M., Liu, F., Huang, Q., Yang, Y., Xiang, P., Lü, Y., and Liu, C. Q. (2018), Importance of considered organic versus inorganic source of carbon to lakes for calculating net effect on landscape C budgets. *J. Geophy. Res. Biogeosci.*, 123(4), 1302-1317. doi: 10.1002/2017JG004159.

MacIntyre, S. (1993), Vertical mixing in a shallow, eutrophic lake: Possible consequences for the light climate of phytoplankton. *Limnol. Oceanogr.*, 38(4), 798-817. doi: 10.4319/lo.1993.38.4.0798.

MacIntyre, S., Eugster, W., and Kling, G. W. (2001), The critical importance of buoyancy flux for gas flux across the air-water interface. *Geophy Monograph-American Geophy Uni.*, 127, 135-140. doi:10.1029/GM127p0135.

MacIntyre, S., Romero, J. R., and Kling, G. W. (2002), Spatial-temporal variability in surface layer deepening and lateral advection in an embayment of Lake Victoria, East Africa. *Limnol. Oceanogr.*, 47, 656-671. doi:10.4319/lo.2002.47.3.0656.

Maruya Y., Nakayama, K., Shintani, T., and Yonemoto, M. (2010), Evaluation of entrainment velocity induced by wind stress in a two-layer system. *Hydrol. Res Lett.*, 4, 70-74. doi:10.3178/hrl.4.70.

Mallin, M. A., and Paerl, H. W. (1992), Effects of variable irradiance on phytoplankton productivity in shallow estuaries. *Limnol Oceanogr.*, 37(1), 54-62. doi:10.4319/lo.1992.37.1.0054.

McDonald, C. P., Stets, E. G., Striegl, R. G. and Butman, D. (2013), Inorganic carbon loading as a primary driver of dissolved carbon dioxide concentrations in the lakes and reservoirs of the contiguous United States. *Global Biogeochem Cycles*. 27(2), 285-295. doi:10.1002/gbc.20032.

Nakamoto A., Nakayama, K. Shintani, T., Maruya, Y., Komai, K., Ishida, T., and Makiguchi, Y. (2013), Adaptive management in Kushiro Wetland in the context of salt wedge intrusion due to sea level rise. *Hydrol. Res. Lett.*, 7(1), 1-5. doi:10.3178/hrl.7.1.

Nakayama, K. Shintani, T., Kokubo, K., Kakinuma, T., Maruya, Y., Komai, K., and Okada, T. (2012), Residual current over a uniform slope due to breaking of internal waves in a two-layer system. *J. Geophys. Res.*, 117, C10002. doi:10.1029/2012JC008155.

Nakayama, K., Shintani, T., Shimizu, K., Okada, T., Hinata, H., and Komai, K. (2014), Horizontal and residual circulations driven by wind stress curl in Tokyo Bay. *J. Geophys. Res.* 119(3), 1977-1992. doi:10.1002/2013JC009396.

Nakayama, K., Nguyen, H. D., Shintani, T., and Komai, K. (2016), Reversal of secondary circulations in a sharp channel bend. *Coast. Eng. J.*, 58(02), 1650002. doi:10.1142/S0578563416500029.

Nakayama, K., Sato, T., Shimizu, K., and Boegman. L. (2019), Classification of internal solitary wave breaking over a slope. *Phys. Rev. Fluids*, 4(1), 014801. doi:10.1142/S0578563416500029.

Plummer, L. N., and Busenberg, E. (1982), The solubilities of calcite, aragonite and vaterite in CO_2-H_2O solutions between 0 and 90 °C, and an evaluation of the aqueous model for the system $CaCO_3$-CO_2-H_2O. *Geoch Cosmochimica Acta.,* 46(6), 1011-1040. doi:10.1016/0016-7037(82)90056-4.

Raymond, P. A., Hartmann, J., Lauerwald, R., Sobek, S., McDonald, C., Hoover, M., Butman, D., Striegl, R., Mayorga, E., Humborg, C., Kortelainen, P., Dürr, H., Meybeck, M., Ciais, P., and Guth, P. (2013), Global carbon dioxide emissions from inland waters. *Nature*, 503(7476), 355-359. doi: 10.1038/nature12760.

Read, J. S., Hamilton, D. P., Desai, A. R., Rose, K. C., MacIntyre, S., Lenters, J. D., Smyth, R. L., Hanson, P. C., Cole, J. J., Staehr, P. A., Rusak, J. A., Pierson, D. C., Brookes, J. D., Laas A., and Wu, C. H., 2012. Lake-size dependency of wind shear and convection as controls on gas exchange. *Geophys. Res Lett.*,39(9), L09405. doi:10.1029/2012GL051886.

581 Robertson, D. M.,& Imberger, J. (1994), Lake number, a quantitative indicator of mixing used to
582 estimate changes in dissolved oxygen. *Int. Revue. ges. Hydrobiol. Hydrogra.,* 79(2), 159-176.
583 doi:10.1002/iroh.19940790202.

584 Shade, A., Chiu, C. Y., and McMahon, K. D. (2010), Seasonal and episodic lake mixing
585 stimulate differential planktonic bacterial dynamics. *Microb. Ecol.,* 59(3):546-554.
586 doi:10.1007/s00248-009-9589-6.

587 Smith, S. V. (1985), Physical, chemical and biological characteristics of CO_2 gas flux across the
588 air-water interface. *Plant, Cell Environ.*, 8(6), 387-398. doi:10.1111/j.1365-
589 3040.1985.tb01674.x.

590 Sobek, S., Algesten, G., Bergstrom, A. K., Jansson, M., and Tranvik, L. J. (2003), The catchment
591 and climate regulation of pCO2 in boreal lakes. *Glob. Change Biol.*, 9(4), 630-641.
592 doi:10.1046/j.1365-2486.2003.00619.x.

593 Staehr, P, & Sand-Jensen K., (2007), Temporal dynamics and regulation of Lake Metabolism.
594 *Limnol. Oceanogr.*, 52(1), 108-120. doi: 10.4319/lo.2007.52.1.0108.

595 Striegl, R. G., Kortelainen, P., Chanton, J. P., Wickland, K. P., Bugna, G. C.,and Rantakari, M.
596 (2001), Carbon dioxide partial pressure and 13C content of north temperate and boreal lakes at
597 spring ice melt. *Limnol. Oceanogr.*, 46, 941-945. doi:10.4319/lo.2001.46.4.0941.

598 Stumm, W., and Morgan, J. J. (1996), Aquatic Chemistry. Chapter 6-9. Wiley.

599 Tsai, J. W., Kratz, T. K., Hanson, P. C., Wu, J. T., Chang, W. Y., Arzberger, P. W., Lin, B. S.,
600 Lin, F. P., Chou, H. M., and Chiu, C. Y. (2008), Seasonal dynamics, typhoons and the regulation
601 of lake metabolism in a subtropical humic lake. *Fresh. Biol.* 53(10), 1929-1941.
602 doi:10.1111/j.1365-2427.2008.02017.x.

603 Tsai, J. W., Kratz, T. K., Hanson, P. C., Kimura, N., Liu, W. C., Lin, F. P., Chou, H. M., Wu, J.
604 T. and Chiu, C. Y. (2011), Metabolic changes and the resistance and resilience of a subtropical
605 heterotrophic lake to typhoon disturbance. *Can. J. Fish. Aquat. Sci.* 68(5), 768-780.
606 doi:10.1139/f2011-024.

607 Tsai, J. W., Kratz, T. K., Rusak, J. A., Shih, W. Y., Liu, W. C., Tang, S. L., and Chiu, C. Y.,
608 (2016), Absence of winter and spring monsoon changes water level and rapidly shifts
609 metabolism in a subtropical lake. *Inland Waters*, 6(3), 436-448. doi:10.1080/IW-6.3.844.

610 Tonetta, D., Staehr, P. A. and Petrucio, M. M., 2017. Changes in CO2 dynamics related to
611 rainfall and water level variations in a subtropical lake. *Hydrobiologia*, 794, 109-123. doi:
612 10.1007/s10750-017-3085-7.

613 Tokoro, T., Hosokawa, S., Miyoshi, E., Tada, K., Watanabe, K., Montani, S., Kayanne, H.,
614 Kuwae, T. (2014), Net uptake of atmospheric CO2 by coastal submerged aquatic vegetation.
615 *Glob. Change. Biol.*, 20(6), 1873-1884. doi: 10.1111/gcb.12543.

616 Typhoon data base of Central Weather Bureau in Taiwan (CWBT),
617 https://rdc28.cwb.gov.tw/TDB/.

618 Vachon, D., and del Giorgio, P. A. (2014), Whole-lake CO_2 dynamics in response to storm
619 events in two morphologically different lakes. *Ecosystems*. 17(8), 1338-1353.
620 doi:10.1007/s10021-014-9799-8.

Verpoorter, C., Kutser, T., Seekell, D. A., and Tranvik. L. J. (2014), A global inventory of lakes based on high-resolution satellite imagery. *Geophys Res. Lett.* 41(18), 6396–6402. doi:10.1002/2014GL060641.

von Robertson, D. M., & Imberger, J. (1994), Lake number, a quantitative indicator of mixing used to estimate changes in dissolved oxygen. Internationale Revue der gesamten *Hydrobiol. Hydrogra*, 79(2), 159-176. doi: 10.1002/iroh.19940790202.

Wanninkhof, R. (1992), Relationship between wind speed and gas exchange over the ocean. *J. Geophys. Ress Oceans.*, 97(C5), 7373-7382. doi: doi.org/10.1029/92JC00188.

Weyhenmeyer, G. A., Kosten, S., Wallin, M. B., Tranvik, L. J., Jeppesen, E., and Roland, F. (2015), Significant fraction of CO_2 emissions from boreal lakes derived from hydrologic inorganic carbon inputs. *Nature Geosci.,* 8(12), 933-936. doi:10.1038/ngeo2582.

Wu, J. T., Chang, S. C., Wang, Y. S., Wang, Y. F., and Hsu, M. K. (2001), Characteristics of the acidic environment of the Yuanyang Lake (Taiwan). *Bot. Bull. Acad Sin.*, 42, 17-22.

Xu, Z., & Xu, Y. J. (2018), Dissolved carbon transport in a river-lake continuum: A case study in a subtropical watershed, USA. *Sci. Total Environ.*, 643, 640-650. doi:10.1016/j.scitotenv.2018.06.221.

638 **Figure 1**. Location of Taiwan with an enlarged bathymetric map of Yuan-Yang Lake (YYL)
639 drawn with 1.0, 2.0, 3.0, and 4.0 m water depths contour lines. Station A (St. A) for vertical
640 profiles (Black Square), 6 river (Red circles) and outflow (Black circle) deployment sites.

641 **Figure 2**. **(a)** Definition of intrusion depth (Zintru.) and mixing depth (Zmix). **(b)** Bathymetry in
642 YYL. Triver is water temperature from the rivers.

643 **Figure 3**. Overview of the vertical profiles of mean water temperature (colors solid lines) and
644 DIC (black dashes) during **(a)** spring, **(b)** summer, **(c)** autumn **(d)** winter **(e)** summer typhoons
645 **(f)** autumn typhoons over the period July 2004 to December 2017. The dots show mean value,
646 the horizontal lines standard deviation (n is samples size).

647 **Figure 4**. Comparison of **(a)** water temperatures and **(b)** DIC concentrations among surface
648 (0.04 m, red bars), bottom (3.5 m, blue bars), and river water (Triver and DICR, green bars). The
649 color bars show mean values and black solid line the standard deviations.

650 **Figure 5**. Comparison of the **(a)** mixing depth, **(b)** Brunt–Väisälä frequency, and **(c)** intrusion
651 depth among the seasons in YYL. The color bar are mean values and the solid black lines the
652 standard deviations. The intrusion depth and mixing depth are normalized by total water depths.

653 **Figure 6**. Relationship between water surface temperatures and **(a)** water surface DIC. **(b)**
654 Hypolimnion DIC, **(g)** Brunt–Väisälä frequency, **(h)** mixing depth; **(c)** is relationship between
655 Hypolimnion DIC and River DIC; and relationship between Brunt–Väisälä frequency and **(d)**
656 water surface DIC, **(e)** Hypolimnion DIC, **(f)** River DIC, **(i)** mixing depth. The green points
657 show spring data; red points the summer data; yellow points the autumn data; blue points the
658 winter data; red crosses the summer typhoon data; and the blue crosses the autumn typhoon data.

659 **Figure 7**. Mean vertical profiles Δ DIC during **(a)** spring, **(b)** summer **(c)** autumn **(d)** winter **(e)**
660 summer typhoons, and **(f)** autumn typhoons.

661 **Figure 8**. Simulation scenarios of a tracer in summer. **(a)** 1st day 00:00 a.m. **(b)** 2nd day 00:00
662 a.m. **(c)** 3rd day 00:00 a.m. X-axis is horizontal distance (m); Y-axis is water depth (m) from
663 bottom to water surface. Contour are drawn to show the concentration of the tracer.

664 **Figure 9**. Contribution of NEP in YYL (excluding the typhoon periods). Carbon is absorbed
665 when NEP > 0 was; carbon releases when NEP < 0.

666 **Figure 10**. Schematic diagrams of stratification **(a)** in spring and summer **(b)** in autumn **(c)** in
667 winter, and (d) after typhoons. The horizonal while-dash line is the boundary of stratification, the
668 vertical yellow line is the DIC concentration, and the vertical yellow-dash line is DICR.
669

670 **Table 1.** Vertical profile of water volumes in YYL.

671 **Table 2.** Spearman correlation coefficients for DIC concentration, water temperature, Brunt-
672 Väisälä frequency, and intrusion depth. BVF is Brunt-Väisälä frequency. WT (0.04 m) is water
673 surface temperature.

674 **Table 3.** The estimated residence time (tr) among seasons.

675 **Table 4.** Characteristics of precipitation and wind speed between summer and autumn typhoon
676 periods during 2004 to 2017.

677 **Table 5.** Equations and references of CO_2 flux (FCO_2) across the air–water interface. Measured
678 data was located St. A.

679 **Table 6.** CO_2 flux in YYL during July 2011 to December 2017 (not including 2012 and 2013).
680 Fc is carbon emission.
681